Reducing Background Contributions in Fluorescence Fluctuation Time-Traces for Single-Molecule Measurements in Solution

Zeno Földes-Papp*, Shih-Chu Jeff Liao, Tiefeng You and Beniamino Barbieri

ISS, 1602 Newton Drive, Champaign-Urbana, IL 61822, USA

Abstract: We first report on the development of new microscope means that reduce background contributions in fluorescence fluctuation methods: i) excitation shutter, ii) electronic switches, and iii) early and late time-gating. The elements allow for measuring molecules at low analyte concentrations. We first found conditions of early and late time-gating with time-correlated single-photon counting that made the fluorescence signal as bright as possible compared with the fluctuations in the background count rate in a diffraction-limited optical set-up. We measured about a 140-fold increase in the amplitude of autocorrelated fluorescence fluctuations at the lowest analyte concentration of about 15 pM, which gave a signal-to-background advantage of more than two-orders of magnitude. The results of this original article pave the way for single-molecule detection in solution and in live cells without immobilization or hydrodynamic/electrokinetic focusing at longer observation times than are currently available.

Keywords: Single-molecule fluorescence fluctuation spectroscopy and imaging, solution, fluorescence correlation, FCS, scattered background, Raman and Rayleigh stray light, autofluorescence, pulsed excitation, modulated excitation, detector gating, time-correlated single-photon counting, TCSPC, early and late time gating, fluorescence lifetime.

INTRODUCTION

Fluorescence fluctuation methods, atomic force microscopy (AFM) with single atomic resolution and mass spectrometry, with atomic unit resolution, are the most sensitive analytical tools in the life sciences and biochemistry [1, 2]. They also allow for direct observations of single molecules. Even though single-molecule observations on immobilized molecules are becoming a standard laboratory technique [2], the measurements on single molecules in solution or in a live cell are a cutting edge technology. It is still a challenging and open task to measure an individual molecule freely diffusing in solution in the upper millisecond and second time regimes with today's instrumentation.

Detectors achieve photon detection efficiencies near 0.7 with very low electronic noise (dark current). For example, the sample fluorescence is recorded with EG&G-Perkin Elmer avalanche photodiodes, which measure the precise time delay between excitation and emission for millions of photon events. A new generation of multichannel discrete-amplification photon detectors (DAPD) devices have begun to rival the photonmultiplier tube with many parameters comparable to or even better than those of the vacuum-tube devices [3]. Interference filters block Rayleigh scattering with extremely high optical densities and are nearly transparent for the chosen fluorescence emission wavelength. The development of microscope objectives with high numerical aperture (N.A.) has represented a significant contribution to the field of ultrasensitive fluorescence detection as well. The fluorescence collection efficiency is determined by the N.A. of the microscope objective. The highest achievable N.A. equals the refractive index of the medium from which the signals are collected, for example 1.33 for the fluorescence collected inside water and 1.52 for fluorescence collected from the surface of a microscope coverslip. The refraction index of a live cell is typically 1.38. A drawback of the very high aperture objectives (N.A. > 1.4 for oil immersion objectives) is that spherical aberrations occur at large angles. For a 1.45 N.A. microscope objective, it is virtually impossible to balance spherical and chromatic aberrations and achieve diffraction limited performance within a large field of view. Therefore, the use of very high aperture objectives is limited to total internal reflection fluorescence (TIRF) wide-field imaging but they should be avoided for confocal microscopy. The development of parabolic mirror objectives (PMOs) for total internal reflection fluorescence (TIRF-PMO) and for supercritical angle fluorescence (SAF-PMO) can overcome a problem of generating diffraction limited detection volumes at large detection angels, which thereby motivates their use in fluorescence correlation spectroscopy (FCS) at surfaces but not in solution. The TIRF-PMO and SAF-PMO generates detection volumes of a few attoliter. With the confocal TIRF-PMO the surface is illuminated exclusively above the critical angle restricting the excitation intensity to the direct vicinity of the coverslip. With the confocal SAF-PMO objective the fluorescence signal is collected exclusively above the critical angle, achieving a comparably fast decay of the detection volume into the analyte solution [4]. This is an alternative approach to Hell and co-workers who used conventional objectives and generated fluorescence detection volumes in solution and at surfaces that are even in the sub-attoliter range [5-7]. Data on single fluorophore detection in nanochannels with burst rates at 1 MHz level were reported in ref. [8] by using a conventional 0.9 N.A. microscope objective. The confinement of the fluorophore in the nanochan-

*Address correspondence to this author at the Visiting professorships at ISS and at the Department of Molecular Biology and Immunology, Health Science Center, University of North Texas, USA;
E-mail: Zeno.Foldes-Papp@medunigraz.at

1389-2010/09 $55.00+.00

nel reduced the background signal. From those data, a reasonable conclusion is that conventional microscope optics is capable of detecting high burst rates if background contributions are minimized.

Because of background rejection in a small detection volume, confocal microscopy is the optical platform of choice for FCS [9, 10]. In order to achieve detection sensitivity at the 'single-molecule level', the count rate per molecule per second (CPM) is an important parameter [9-11] as well, but background rejection influences the amplitude of the correlation function [9-12]. For example, the 'background' of high concentrations of autofluorescent molecules can easily hide the low signal from the specific fluorescent molecules and makes weak fluorescence signals extremely difficult to detect. A direct extrapolation from a millisecond to a second time binning is more difficult to perform when photobleaching and triplet crossing influence an evaluation. Under such experimental conditions, it is not possible to extract the CPM from the measurement and a more appropriate measure is the signal-to-background ratio. A lack of diffraction limited optics is usually not a problem in normal FCS; the detection volumes are often enlarged in order to have time for studying different biophysical and biochemical reactions. However, an enlarged detection volume hampers the observation of just one single molecule in solution [12-15].

Fluorescence fluctuation methods such as FCS are sophisticated physical methods. We measure spontaneous fluctuations in a number of molecules within a small illuminated volume of less than one femtoliter. The apparent characteristic diffusion fluctuations might take a characteristic period of time, e.g. a millisecond, but it does not matter how precisely we measure the individual fluctuations, we still cannot get the kinds of parameters such as rate constants that we are interested in. We have to measure many fluctuations and then we analyze the emitted fluorescence fluctuations from that particular measurement. In FCS, we correlate the fluorescence fluctuations and obtain, for example, the diffusion fluctuations for a diffusion process [10]. Analysis tools such as burst size distribution [16], photon-counting histogram (PCH) [17] and fluorescence intensity distribution (FIDA) [18] establish the brightness parameter from the statistics of the amplitude (number of photons) of the fluorescence fluctuations. In fluorescence cross-correlation spectroscopy (FCCS) [19-21] and two-dimensional fluorescence intensity distribution (2D-FIDA) [22] or dual-color PCH [23], the second dimension provides coincident information from a second detector, which may represent a different color or a different fluorescence polarization.

Detecting fluorescence fluctuations from a single molecule is mainly an issue of background reduction rather than detection sensitivity because several millions of photons per second can be emitted by a single fluorophore [24, 25]. In fluorescence fluctuation methods, the fluctuations are measured against a *background noise of Raman and Rayleigh scattered light* from the medium or high dark current of the detector. The first approach that enabled measuring single fluorescent molecules in solution was called time-gated discrimination [26, 27]. The detector was on only for a controlled time interval during a possible fluorescent burst from a single molecule. In the case of Raman scattering, a frequency shift of the light compared to the frequency of the incident light occurs. If an excitation laser has the wavelength λ_0 then the Raman scattered wavelength is [28]

$$\lambda_R = \frac{1}{\left(\frac{1}{\lambda_0} - \hat{\nu}\right)}, \quad (1)$$

where $\hat{\nu}$ is the wavenumber in cm^{-1} characteristic of the medium (solvent, solution). The Raman scattering is a much faster event that the lifetime of a fluorescent dye. Raman scattering generated in the detection volume can be spectrally filtered. In Rayleigh scattering (elastic scattering), the molecule is excited to a virtual state and than relaxed to the same vibrational state. A photon with the same wavelength as the incident light is emitted. In this process, no energy is absorbed by the molecule. Electronic early time-gating discriminates between which photons are incorporated in the analysis based on the time-delay between excitation of the fluorophore and emission of the fluorescence photon as first shown in ref [29]; the detector recorded the fluorescence bursts for a controlled time interval, e.g. in very large detection volumes of picoliters [29-31]. It is now performed entirely in software by using a time-correlated single-photon counting (TCSPC) card for data collection as shown in [32, 33] and by others. In order to time-gating away Rayleigh scattering, the time-gate is chosen to start at a time where the amplitude of the excitation pulse is substantially decreased, e.g. at 2.3 nanoseconds after excitation.

The purpose of this original article was to explore different new microscope means in order to reject background contributions. In particular, we studied the effects of i) excitation shutter, ii) electronic switches, and iii) early and late time-gating with TCSPC on the amplitude of correlated fluorescence fluctuation traces. Low-light applications such as single-molecule observation in biology and chemistry require single-photon sensitivity and very fine timing resolution of detected photons because we want to measure the fluctuations from one individual molecule only. Until now, this has not been possible for more than some milliseconds in solution without hydrodynamic/electrokinetic flow or systemic drift. One major challenge in using extended observation (measurement) scales is still the background contributions from the highly pure and photobleached solvent.

EXPERIMENTAL SECTION

Optical Set-Up

The optical systems were set up on an ALBA-Fluorescence Fluctuation System platform (ISS, Champaign, IL) equipped with a laser scanning unit. A detailed description is given in ref [9]. We collected fluorescence fluctuation data using a 635-nm epifluorescence laser diode source (see section Results and Discussion) and a cooled avalanche photodiode (Model SPCM-AQR-15, by EG&G PerkinElmer, Vaudreuil, Quebec, Canada). Controlling and recording a mechanical shutter and electronic switches of excitation laser and detector required that the devices were synchronized with the laser diode illumination and the avalanche photodiode. The excitation wavelength of the pulsed laser was 635 nm with 39 ps pulse width and 50 MHz repetition rate. The

light was delivered to the microscope through a single mode, 3.5 μm fiber. A Nikon water immersion objective, 60X, N.A. = 1.2 was used. A single-color dichroic filter (633 nm SP Laser Set, Chroma Technology, Rockingham, VT) accepted the 635 nm laser line and reflected above 665 nm. The fluorescence light emitted by the sample travelled back through the scanning mirrors unit. With the long pass filter HQ665lp (Chroma Technology, Rockingham, VT), the emission was directly separated into the channel 1 detector. The measurement time was 50 s with a sampling frequency of 100 KHz resulting in a binning time of 10 μs.

The principle of confocal microscopy is the use of a prefocusing lens that focuses the incoming laser beam to a small spot *A* [9]. This spot is then focused by the microscope lens to an even smaller spot A'. The sample will be illuminated by this very small spot A' with ω about 0.25 μm, where ω is the radial distance before the laser intensity has fallen to $e^{-2} \approx 0.14$. The fluorescence light from this small spot is then collected back through the microscope and focused on the third spot A''. At this position a pinhole is inserted to remove fluorescence light originating from molecules not in focus A' [9]. If the fluorescence light originates below or above A', a large amount of the light not originating from A' will be blocked and not detected by the detector. In this way, depth discrimination is achieved. By using a dichroic mirror, the fluorescence light is separated from the excitation light because the fluorescence light has a longer wavelength than the excitation light. A bandpass filter is inserted between the dichroic mirror and the detector to remove scatted background light.

Signal to Background in Fluorescence Fluctuation Experiments

For a random Poisson process, the fluctuations in a physical parameter such as the number of molecules δN about the average parameter value $\langle N \rangle$ is given by the variance of the process

$$\left\langle (\delta N)^2 \right\rangle = \langle N \rangle \ . \tag{2}$$

Since the fluorescence intensity *I* is directly proportional to *N*, we have the following physical properties

$$\langle I \rangle = i \cdot \langle N \rangle \ , \tag{3}$$

$$\left\langle (\delta I)^2 \right\rangle = i^2 \cdot \left\langle (\delta N)^2 \right\rangle = i^2 \cdot \langle N \rangle , \tag{4}$$

and

$$\frac{\left\langle (\delta I)^2 \right\rangle}{\langle I \rangle^2} = \frac{1}{\langle N \rangle} \ , \tag{5}$$

where *i* is a multiplier (proportionality constant). The random process of fluorescence intensity fluctuations has as many deviations δI below the mean as above it and, therefore, we get $\langle \delta I \rangle = 0$. Hence, the autocorrelated fluorescence fluctuations *G'* at correlation time $\tau = 0$ is given by

$$G_0' = 1 + \frac{\left\langle (\delta I)^2 \right\rangle}{\langle I \rangle^2} = 1 + \frac{1}{\langle N \rangle} \ , \tag{6}$$

as first shown in ref. [34]. Thus, the amplitude minus one of the normalized autocorrelation function at $\tau = 0$ equals the inverse average number of molecules in the small (e.g., femtoliter-sized) observation volume. Here, we consider diffusive processes and not excitation into triplet states. Usual concentrations that can be measured with this approach are between 10^{-8} M and 10^{-11} M. Concentrations at 10^{-8} M give very small amplitudes, whereas concentrations as low as 10^{-11} M require very long measurement times.

Now, $G_0' - 1 = G_0$ is related to the signal N_0 and background *B* as first reported in ref. [35]

$$\frac{1}{\tilde{N}} = \frac{N_0}{(N_0 + B)^2} \ , \tag{7}$$

where $\tilde{N}$ is the 'apparent' number of molecules. We omit the average symbol $\langle \ \rangle$ in equation (7) and the following equations. In principle, there is no need to calibrate the concentration or instrument sensitivity because Eqns. (6) and (7) are determined without any assumption, except that the solution contains a fluorophore. Another important feature of Eqns. (6) and (7) is that they do not depend upon the brightness of the fluorophore. However, the brightness affects the signal-to-background ratio of the measurement and the ability to see the fluorophore over the background [1]. In aqueous solution of a fluorophore, Rayleigh (elastic) and Raman (inelastic) scattering of the solvent are the main sources of background *B* because the detector noise (dark current) can be as low as 25 photon counts by using a cooled avalanche photodiode (Model SPCM-AQR-15, by EG&G PerkinElmer, Vaudreuil, Quebec, Canada).

We first present here the derivation of a more convenient formula than Eqn. (7) [35] for background *B* correction and apply it in the detection of molecule numbers. For this purpose, N_0 is given by the number of specific fluorescent molecules and *B* is given by the number of background counts per molecule. We consider the measured quantities total, *average* fluorescence intensity I_S and *average* background intensity I_B. Then, the number of counts per molecule is

$$N_m = \frac{I_S - I_B}{N_0} \tag{8}$$

and the number of background *B* counts per molecule is

$$B = \frac{I_B}{N_m} = \frac{N_0 \cdot I_B}{I_S - I_B} \ . \tag{9}$$

Hence, the quantitative relationship between the number of molecules N_0 and the amplitude of the autocorrelation function minus one, $\frac{1}{\tilde{N}}$ (Eqn. (6)), becomes

$$\frac{1}{\widetilde{N}} = \frac{N_0}{\left(N_0 + \frac{N_0 \cdot I_B}{I_S - I_B}\right)^2} \quad . \tag{10}$$

Eqn. (10) yields the final expression used for background correction of the measured apparent number $\widetilde{N}$ of molecules in the autocorrelated fluctuation data for all practical purposes [9]

$$N_0 = \frac{\widetilde{N}}{\left(1 + \frac{I_B}{I_s - I_B}\right)^2} \quad , \tag{11}$$

where $\widetilde{N} = \frac{1}{G(0)}$. The formula (Eqn. (11)) assigns directly measured quantities to 'true' values of molecule numbers N_0 corrected for background contributions *B*, which is its advantage over the equation (7). If the background count is more than 100-fold lower than the signal count, then $N_0 \cong \widetilde{N}$. In this way, a high signal-to-background count ratio corrects for background contributions. Therefore, we used a Cy5 stock solution for the dilution experiments, i.e. a high average number of molecules per observation volume, at which the high signal-to-background count ratio corrected itself for background.

Models of the Autocorrelation Function that Describes the Scattered Background Rejection

The scattered light can have the same wavelength as the excitation light, if it is Rayleigh scattered, or be shifted if it is Raman scattered. A fast component of a collected fluorescence process is Raman scattering and fluorescent light. We reject the scattered component by implementing time-windows *T* that are greater than the dynamics of interest τ_{diff} (diffusion)

$$G(\tau) = G_{diff}(0) \cdot diff + G_{\exp}(0) \cdot \exp\left\{-\frac{\tau}{T}\right\} \quad , \tag{12}$$

$$diff = \frac{1}{1 + \frac{\tau}{\tau_{diff}}} \cdot \sqrt{\frac{1}{1 + \frac{\tau}{s^2 \cdot \tau_{diff}}}} \quad , \tag{13}$$

$$s^2 = \left(\frac{z}{\omega_{x-y}}\right)^2 , \tag{14}$$

$$\frac{1}{G_{diff}(0)} = \frac{\overline{N}}{f} = N \quad , \tag{15}$$

$$\frac{1}{G_{\exp}(0)} = \frac{\overline{N}}{1-f} \quad , \tag{16}$$

$$T = \left(k_{on}^{switch} + k_{off}^{switch}\right)^{-1} \quad . \tag{17}$$

f is the fraction of the amplitude $G(0)$ that relates to a molecule number *N*. For slow rates k^{switch} of the switches, $N \cong N_0$. *s* is the structure parameter, which is determined by the dimension of the volume element, i.e. the half-length *z* and the axial radius ω_{x-y} of the focal plane. *diff* is the diffusion term in the autocorrelated data with the diffusion time τ_{diff} of the fluorophore. In the presence of autofluorescence, for example form endogenous fluorescent molecules in a 140 mM NADH solution, we immediately get from Eqn. (12)

$$G(\tau) = \frac{1}{N} \cdot \left[f \cdot \left[(1-Y) \cdot diff_2 + Y \cdot diff_1 \right] + (1-f) \cdot \exp\left\{-\frac{\tau}{T}\right\} \right] \tag{18}$$

where a fraction of all molecules relates to the background rejection term *f* by the time-window *T* applied (optical switch). The $diff_1$ term stands for the fluorophore and the $diff_2$ term for the autofluorecence. The origin of the autofluorescence that we observed may not be due to NADH itself but is probably due to fluorescent 'contaminants' in the concentrated NADH solution. This approach does not reduce in any way the value of the demonstration because we simply used it as a fluorescence background signal (see section 'Results and Discussion', subsection 'Early and late time-gating in the presence of autofluorescence'). Assuming an alternative model, by which the $diff_2$ term was also gradually suppressed by the optical switch *T*, was not in agreement with the measured data.

By means of an iterative least-square algorithm (Marquart algorithm) the model values were compared to the experimental values and approximated until the differences between the two curves were minimized. Each amplitude value of the autocorrelated fluorescence fluctuation traces was the average of 5 million data points. The best mathematical approximation with the smallest degree of error was taken as the final result yielding a chi-square value close to 1.0. Thus, the data were represented by the theoretical curve with a minimum deviation from the measured correlation curve. In this way, we proved that our model equations (12) and (18) fitted the experimental data.

RESULTS AND DISCUSSION

Background contributions in a highly pure aqueous solution (Fluka, Water TraceSELECT®, total evapn. residue guarantee ≤ 0.0001 %) of a fluorophore Cy5 that was used throughout this study mainly consist of out-of-focus fluorescence light and scattered light. Out-of-focus fluorescence light was removed using the pinhole (see subsection Optical Set-Up, confocal set-up). Some of the scattered light was removed using optical bandpass and interference filters (see Experimental Section, subsection Optical Set-Up). When fluorescent light is collected, optical bandpass filter and interference filters remove wavelengths that are not in the fluorescent range. But even the most excellent optical components cannot reject background contributions completely. For

example, the Stokes-shifted Raman scattered light can have spectral components in the fluorescent range.

Comparison of Correlated Fluorescence Fluctuation Traces without and with Mechanical Excitation Shutter

The laser power was 40 μW measured at the exit of the objective. In Fig. (**1**), we demonstrate how an excitation shutter rejected background-signal contributions. The time traces contained photon bursts, which were equally distributed in time (Fig. **1A**). The photon bursts originated from the fluorophore Cy5 and from background contributions in aqueous solution. Scattered light that remained after optical bandpass and interference filters was removed by applying an additional longer time window of off-times during the measurement (Fig. **1B**) resulting in less background contributions and, therefore, in an increased G(0) value (Fig. **1D**) compared to the values without excitation shutter (Fig. **1C**). After cutting-off all the shutter's off-times by data processing (Fig. **1E**), we obtained a lower G(0) value (Fig. **1F**), which was fairly the same as the G(0) value without excitation shutter (Fig. **1C**). The time-dependent part of the autocorrelated fluorescence fluctuation data obtained from the aqueous Cy5 solution in the presence of the excitation shutter was superimposed by the slow frequencies of on- and off-times of 1 Hz as shown in the insert of Fig. (**1D**). Applying the two independent models of Eqn. (11) and Eqns. (12) – (17) to the data shown in Fig. (**1**), the background-corrected molecule numbers were in good agreement between the different data analyses: N_0 = 0.787 arising from the treatment by Eqn. (11) in Fig. (**1C**), N_0 = 0.767 due to the treatment by Eqns. (12) – (17) in Fig. (**1D**), and N_0 = 0.777 arising from the treatment by Eqn. (11) in Fig. (**1F**). Both data treatments are merely an alternative way of correcting background contributions, which yield fairly the same N_0 values when properly performed. Autocorrelation of fluorescence time-traces provides a measurement of the average number of molecules in the observed volume, even if the bulk concentration is not known.

Comparison of Correlated Fluorescence Fluctuation Traces without and with Electronic Switches

The laser power was 50 μW measured at the exit of the objective. A series of measurements were made at higher concentrations of the fluorophore Cy5 and compared with a series with electronic switches at 0.5 Hz. Table **1** shows that modulated excitation [36] by an electronic switch could be employed, as expected, at low fluorophore concentration of about 0.17 nM when the background count is less than 100-fold lower than the signal count. At N/1000, modulated excitation with $T >> \tau_{diff}$ brings advantage under conditions with scattered light or high dark current because the simple relation $N = 1/G(0)$ is not applicable due to stray light or high dark current. Only here the model (12)-(17) can offer more robust data analysis by separating the different processes from each other. This results in accurate average molecule number $N \cong N_0$ during measurement as shown in the last row of Table **1**. Additional synchronized time-gating of the detector decreased the fluorescence intensity incorporated in the autocorrelation analysis and can also lead to an increase in the amplitude of the fluctuations, but did not yield an overall improvement in the signal-to-background ratio as first shown in the last column of Table **1**.

Comparison of Correlated Fluorescence Fluctuation Traces with Early and Late Time-Gating

Scattered light is a fast process compared with the excitation and fluorescent relaxation process. By using pulsed lasers with short pulses, e.g. 39 ps pulse width and 50 MHz repetition rate, most of the Rayleigh scattering will occur as long as the pulse duration. Because the data are stored in the time-tagged time-resolved mode that allows for recording every detected photon with its individual timing and detection channel information, it is possible to detect photons that arrive at the detector some ps after the excitation pulse. In this way, Rayleigh scattered light can be removed by early time-gating [27].

Fluorescence from the fluorophore molecules Cy5 in the laser beam and scattering from solvent are two independent processes. In a time interval, the observed photon counts come from *any combination of scattering and fluorescence*. Hence, the observed distribution of photon counts is the convolution of background scattering *and* fluorescence emission occurring in the observation (measurement) time. This is the physical reason why the mean fluctuation in the background increases linearly with light intensity. In other words, at any time the emission in the detection volume consists of bursts of fluorescence from fluorophore molecules passing through superimposed on a *continuous background* due to Rayleigh and Raman scattering.

For data acquisition, we used here a Single Photon Counting (SPC)-card. The laser power measured at the exit of the objective was 50 μW. In order to check the dilutions of the aqueous Cy5 stock solution, we measured the total fluorescence intensities I_S and the background intensities I_B. After subtracting the background intensities I_B, the mean fluorescence intensities decreased linearly with the sample dilution step until N/100 according to Eqn. (3). At the final dilution step, the mean fluorescence intensity approach was not sensitive enough but the bulk concentration at N/1000 corresponded to even less than 12 pM estimated by the fluorescence fluctuation approach of Fig. (**2**). As shown in Fig. (**2**), we first found conditions of early and late time-gating with TCSPC that made the fluorescence signal as bright as possible compared with the fluctuations in the background count rate in a diffraction-limited optical set-up. The increased amplitude saturated at a certain level of dye dilution indicating that the increase in the amplitudes did not resulted from the electronics of the measurement system (data not shown). With removal of scattering contributions of early and late photons after each excitation pulse during measurement times, we collected a G(0) value of 11.07 at N/1000 compared with a G(0) value of 0.08 at N* (Fig. **2**). Thus, we measured about a 140-fold increase in the amplitude G(0) of

A)

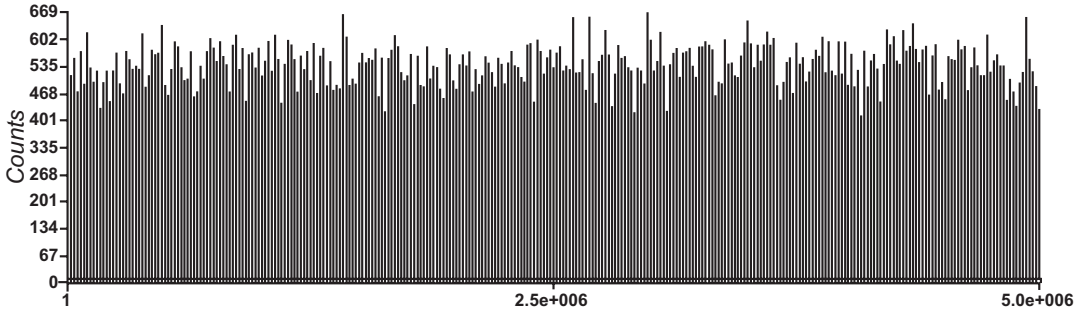
Counts
669
602
535
468
401
335
268
201
134
67
0
1
2.5e+006
5.0e+006

B)

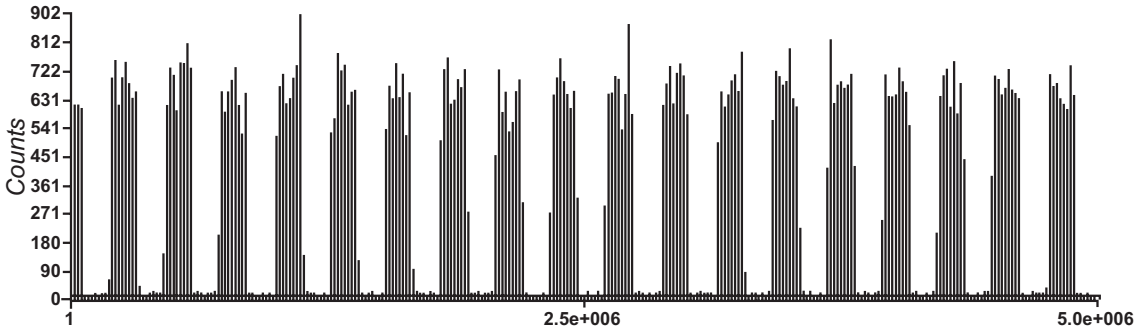
Counts
902
812
722
631
541
451
361
271
180
90
0
1
2.5e+006
5.0e+006

C)

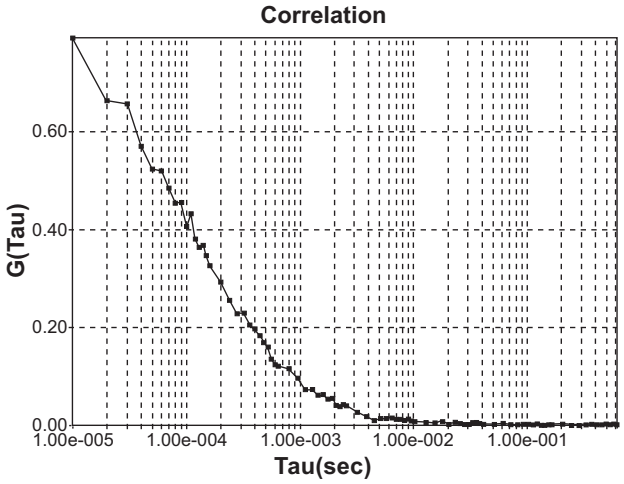
Correlation
G(Tau)
0.60
0.40
0.20
0.00
1.00e-005
1.00e-004
1.00e-003
1.00e-002
1.00e-001
Tau(sec)

D)

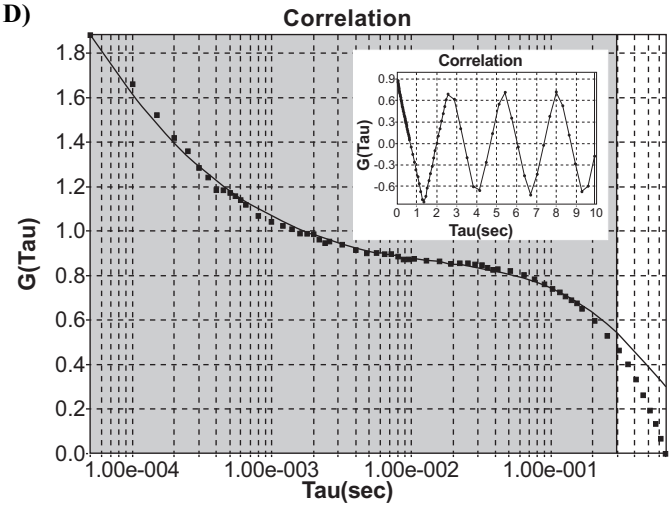
Correlation
G(Tau)
1.8
1.6
1.4
1.2
1.0
0.8
0.6
0.4
0.2
0.0
1.00e-004
1.00e-003
1.00e-002
1.00e-001
Tau(sec)
Correlation
G(Tau)
0.9
0.6
0.3
0.0
-0.3
-0.6
0 1 2 3 4 5 6 7 8 9 10
Tau(sec)

E)

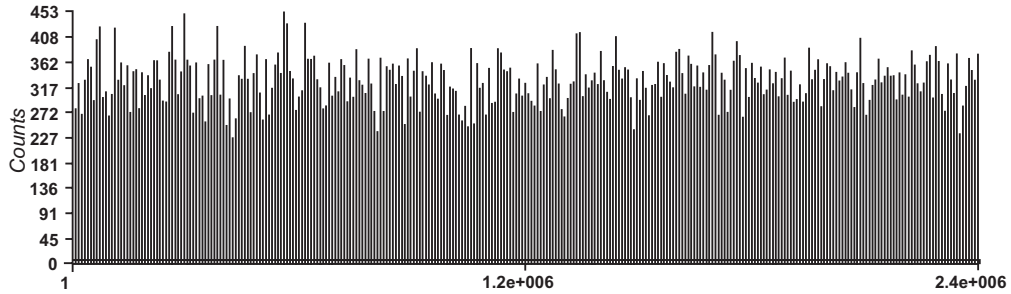
Counts
453
408
362
317
272
227
181
136
91
45
0
1
1.2e+006
2.4e+006

(Fig. 1) contd…

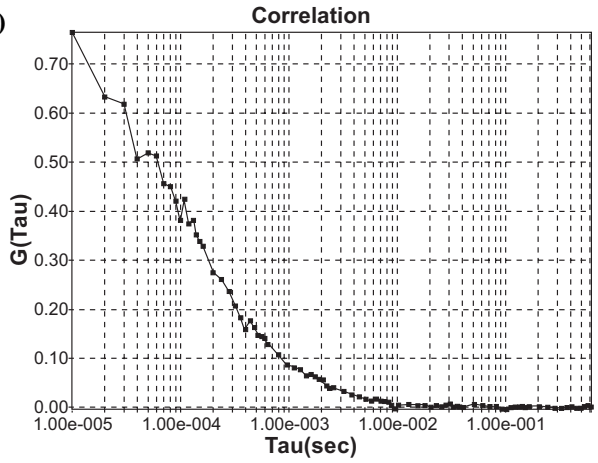

Fig. (1). Fluorescence fluctuation measurements were performed in aqueous solution of Cy5.

A: Measured fluorescence fluctuation time-traces of Cy5 molecules diffusing through the confocal detection volume. No excitation shutter was applied.

B: Measured fluorescence fluctuation time-traces of Cy5 molecules diffusing through the confocal detection volume. An excitation shutter was applied with frequencies of off-times and on-times of 1 Hz each. Thus, the parameter *T*, which quantitatively describes the time window, is $T = \left(k_{on}^{switch} + k_{off}^{switch}\right)^{-1} = 0.5$ s (Eqn. (17)).

C: Autocorrelated data from **A** with the measured value $\frac{1}{G_{diff}(0)} = \widetilde{N} = 1.25$. The measured quantities total fluorescence intensity I_S = 3.871 kHz and background intensity I_B = 0.799 kHz resulted in a background-corrected molecule number N_0 of 0.787 (Eqn. (11)).

D: Autocorrelated data from **B**. The time-dependent part of the autocorrelated fluorescence fluctuation data was superimposed by the slow frequencies of the excitation shutter of 1 Hz as shown in the insert. The theoretical model of Eqns. (12) – (17) (solid line) was in excellent agreement with the observed data points (squares) within the grey range neglecting the shutter oscillations that occurred at a longer time scale than diffusion ($T >>$ the time parameter of the process of interest, i.e. in our study the diffusion time of the fluorophore Cy5). The theoretical model yielded the following parameters for the background-corrected molecule number: $\frac{1}{G_{diff}(0)} = \frac{\overline{N}}{f} = \frac{0.453}{0.591} = 0.767$, where T = 0.569 s was unfixed. Squares, experimental values; solid line, theoretical curve.

E: Data processing of B by cutting the intervals when the shutter was closed (off-times).

F: Autocorrelated data from **E** yielding fairly a similar G(0) value as in **C** with the measured value $\frac{1}{G_{diff}(0)} = \widetilde{N} = 1.30$. The measured quantities total fluorescence intensity I_S = 2.165 kHz and background intensity I_B = 0.491 kHz resulted in a background-corrected molecule number N_0 of 0.777 (Eqn. (11)).

autocorrelated fluorescence fluctuations at the lowest analyte concentration N/1000. Our findings gave a signal-to-background advantage of more than two-orders of magnitude. Early and late time-gating with TCSPC as pioneered in this study for a diffraction-limited optical set-up eliminate background contributions across the measurement time. For comparison with the corresponding data without removing early scatter and late afterglow, we show the amplitudes G(0) of autocorrelated fluorescence fluctuations in the laser-pulsed diffraction-limited optical setup in Fig. (**3**).

In Table **2**, we demonstrate that the background-corrected number of molecules N_0 obtained from the apparent number of molecules $\widetilde{N}$ (Eqn. (11)) containing background contributions equals the measured number of molecules from the reverse amplitude minus one when background contributions were removed by early and late time gating. The total fluorescence intensity I_S was 535 counts per second and the background intensity I_B was 90 counts per second. Considering G(0) without removal of scatter and afterglow, we found $\widetilde{N} = \frac{1}{4.935} = 0.203$. With correction for background by Eqn. (11), we obtained N_0 = 0.1404. Hence, the G(0) should be 1/0.1404 = 7.123, which is very close to what we measured with removal both of scattering and afterglow by early and late time-gating. In fact, N_0 satisfies equation (11). Thus, by the properties of Eqn. (11), we can quantify the background contributions for measured amplitudes of autocorrelated fluorescence intensity traces. In most practical problems, the background contributions are unknown, but Eqn. (11) can be used to directly obtain the correct molecule number from the amplitude of the autocorrelated fluorescence fluctuation time-traces.

Early and Late Time-Gating in the Presence of Autofluorescence

The laser power at the exit of the objective was 50 μW. We used NADH to simulate a biological environment with some autofluorescence. The 140 mM NADH solution gave an autofluorescence contribution of 550 photon counts per second at 635 nm pulsed excitation with a 50 MHz repetition rate. The precise origins of that signal are not clear but we simply used it as a background signal. The observed autofluorescence may be due to spurious fluorescent molecules in the NADH sample. Such a scenario is, in fact, to be expected considering that the NADH sample is 140 mM. We first report data indicating suppression of autofluorescence in fluorescence fluctuation time-traces. In these experiments, a known number of Cy5 molecules plotted in the first column of Table **3** provided the specific signal. Their autocorrelated amplitudes were reduced due to the excess of autofluorescent molecules as seen in the second column of Table **3**. The level of 'recovering' the Cy5 molecules shown as increase in the autocorrelated amplitudes after early and late time-gating is so far very small compared to the signal increase for a Cy5 solution in the absence of autofluorescence depicted in Fig. (**2**). Our approach for real-time suppression of autofluorescence in fluctuation time-traces is based upon lifetime measurements to discriminate between, for example, short-lived autofluorescence (ca. 0.4 ns) and long-lived specific fluorescence (ca. 1 ns) as illustrated in Fig. (**4**). From the life time measurements of the Cy5 and the autofluorescent solutions, we see that removing autofluorescent afterglow

Table 1. Amplitudes G(0) of Autocorrelated Fluorescence Fluctuations. N* = 181.28 of a 170 nM Aqueous Cy5 Solution Diluted from a Cy5 Stock Solution that Corrected for Background Contributions by a High Signal-to-Background Count Ratio (see Experimental Section)

Number of Molecules	G(0) ; *N* No Excitation Shutter and No Detector Gating; No Background Correction was Applied	G(0) ; *N* with Excitation Shutter at 0.5 Hz; Background Correction According to Model (12) − (17) with *T* = 0.25 s	G(0) ; *N* with Synchronized Excitation Shutter and Detector Gating at 0.5 Hz Each; Background Correction According to Model (12) − (17) with *T* = 0.125 s
N*	0.0055 ; 181.28	1.00456 ; 183.35	1.003 ; 172.96
N/10	0.0551 ; 18.16	1.10587 ; 11.503	1.092 ; 12.16
N/100	0.5434 ; 1.84	2.00743 ; 0.982	1.989 ; 1.093
N/1000	3.8375 ; n.a.	7.80403 ; 0.1383[#]	8.685 ; 0.1325[#]

n.a.: The simple relation $N = 1/G(0)$ is not applicable due to stray light or high dark current.

[#]: Only here the model (12) – (17) offers more robust data analysis due to the added possibilities to separate processes from each other.

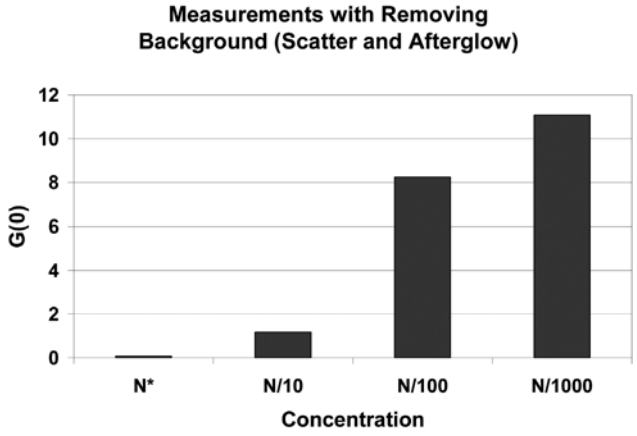

Fig. (2). Amplitudes G(0) of autocorrelated fluorescence fluctuations with removing early scatter within 600 ps (first off-time) after each excitation pulse and afterglow 15 ns later (second off-time) after each excitation pulse. Only photons within this temporal limit of the time-gate were used for data acquisition. N* = 12.24 of a 12.06 nM aqueous Cy5 solution diluted from a Cy5 stock solution that corrected for background contributions by a high signal-to-background count ratio (see Experimental Section).

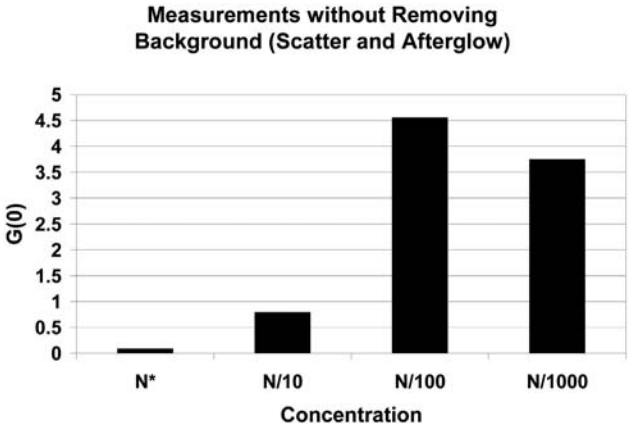

Fig. (3). Amplitudes G(0) of autocorrelated fluorescence fluctuations without removing early scatter and late afterglow in the laser-pulsed diffraction-limited optical setup. N* = 12.24 of a 12.06 nM aqueous Cy5 solution diluted from a Cy5 stock solution that corrected for background contributions by a high signal-to-background count ratio (see Experimental Section).

Table 2. Amplitudes G(0) of Autocorrelated Fluorescence Fluctuations

G(0) without Removal of Background Contributions	G(0) with Early[+] Time-Gating	G(0) with Early[+] and Late[#] Time-Gating (Removal of Scatter and Afterglow)
4.935	5.478	7.547

[+] Scatter is removed by 3% beginning of 20 ns, which is 0.6 ns.

[#] Afterglow is removed by 70% from the end of the 20 ns laser pulse repetition, which is between 14 and 20 ns.

was insufficiently small at the cut-off time of the chosen late time-gating, whereas the chosen early time-gating was too short in order to remove enough autofluorescence photons embedding the weak fluorescence signal. The lifetimes of a mixture of Cy5 and autofluorescent molecules depend very much on the ratio of both components. Because we missed the proper cut-off points for early and late time-gating in contrast to a Cy5 solution without autofluorescence, the resulting effect in autofluorescence background suppression was very small (Table **3**).

Table 3. Different Known Numbers of Cy 5 Molecules with N* = 1.008 Corresponding to 1.5 nM Cy5 in ca. 140 mM NADH Solution[¶]

Known Number of Cy5 Molecules	G(0) without Removal of Background and Autofluorescence Contributions	G(0) with Early[+] and Late[#] Time-Gating (Removal of Scatter and Afterglow)
N*	0.2135	0.19989
N/10	0.9700	1.0506
N/100	0.5441	0.6068

[+] Scatter is removed by 3% beginning of 20 ns, which is 0.6 ns.

[#] Afterglow is removed by 70% from the end of the 20ns laser pulse repetition, which is between 14 and 20 ns.

[¶] The origin of the autofluorescence may not be due to NADH itself but is probably due to endogenous fluorescent molecules in the concentrated NADH solution. Even if the precise origins of that signal are not clear, we simply used it as a background signal. This approach does not reduce in any way the value of the observation at all (see main text).

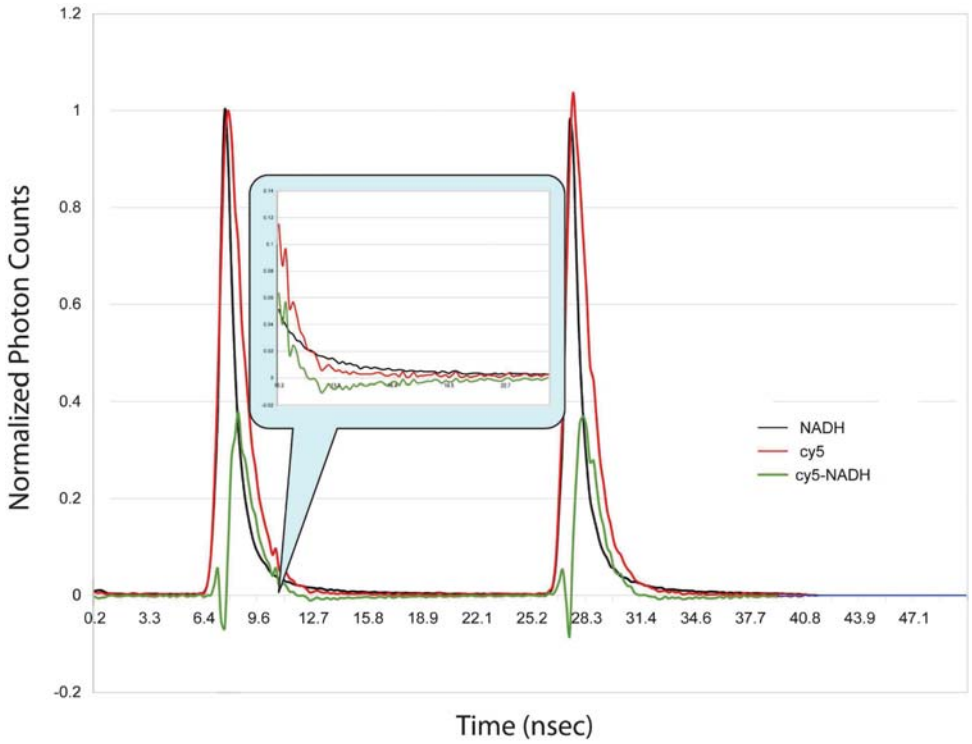

Fig. (4). Histogram of photon arrival times at the detector of Cy5 and endogenous fluorescent background of a concentrated NADH solution.

SUMMARY

Taken together, our new idea and invention is to remove remaining scatter from the solvent, which goes with the fluorescence, by using more than one time window of off-times during the measurement. This physical principle corresponds to early and late time-gating of the arrival of photons in a laser-pulsed diffraction-limited optical set-up if the photons are collected by time-correlated single-photon counting (TCSPC) that give full access to the timing of each photon arrived on the detector. Rejection of background and autofluorescence could only be achieved by early and late time gating in TCSPC mode. We put forward a lifetime approach by which we determined the cut-off time points in the time-tagged photon arrival times. However, the resulting effect was small compared with the effect of early and late time-gating for a Cy5 solution without autofluorescence. The reason is that the lifetimes of a mixture of Cy5 and endogenous fluorescent molecules depend very much on the ratio of both components. That means that we probably missed the right cut-off points in early and late time-gating in contrast to the Cy5 solution without autofluorescence. The background rejection implemented by mechanical and electronic (optical) switches acts on the scattered background or high dark current. Any optical switch T, where T is the operation rate of the switch, can only reject scattered background or high dark current if T satisfy the condition $T >>$ the time parameter of the process of interest, i.e. in our study the diffusion time of the fluorophore. We first report data showing that modulated excitation can result in rejection of scattered background under those conditions. Background rejection by mechanical and electronic (optical) switches does not discriminate between fluorophore and autofluorescence. Assuming an alternative model, by which the autofluorescence was also gradu-

ally suppressed, was not in agreement with the measured data. Background rejection by mechanical and electronic (optical) switches is not in favor of autofluorescence suppression.

CONCLUSIONS

Our obtained results pave the way for single-molecule detection in solution at longer observation times that are currently not available [12-14]. The concentration of the liquid by dilution is so small that the detection volume contains a single molecule or two or three single but different molecules. Their random motions in a liquid solution are detected by recording the fluorescence fluctuations. The time that a single molecule is in the observation volume and the second and third are not can be precisely calculated under such experimental conditions from first physical principles [12]. To study it definitely at the level of single molecule interactions has, up to now, surpassed the capabilities of modern instrumentation. The first true demonstration of a technology leading towards the observation of just one single molecule confined within solution without hydrodynamic/electrokinetic flow is still missing for an extended observation time of more than one millisecond and a couple of milliseconds, respectively [37].

ACKNOWLEDGEMENT

Zeno Földes-Papp acknowledges financial support in part from his FWF Austrian Science Fund Research Project P20454-N13.

REFERENCES

[1] Lakowicz, J.R. (2006) *Principles of fluorescence spectroscopy.* 3rd ed., Springer, New York.

[2] Selvin, P.R. and Ha, T., Eds. (2007) *Single-molecule techniques: a laboratory manual.* Cold Spring Harbor Laboratory Press, Cold Spring Harbor, New York, USA.

[3} Linga, K. (2008) Discrete amplification dramatically improves single-photon detection. *Laser Focus World,* **44** (12), 51-53.

[4] Ruckstuhl, T. and Verdes, D. (2004) Supercritical angle fluorescence (SAF) Microscopy *Opt. Express,* **12** (18), 4646-4654.

[5] Klar, T.A.; Jakobs, S.; Egner, A. and Hell, S.W. (2000) Fluorescence microscopy with diffraction resolution barrier broken by stimulated emission. *Proc. Natl. Acad. Sci. USA*, **97** (15), 8206-8210.

[6] Dyba, M. and Hell, S.W. (2002) Focal spots of size lambda/23 open up far-filed fluorescence microscopy at 33 nm axial resolution. *Phys. Rev. Lett*., **88**, 163901.

[7] Dyba, M.; Jakobs, S. and Hell, S.W. (2003) Immunofluorescence stimulated emission depletion microscopy. *Nat. Biotechnol*., **21** (11), 1303-1304.

[8] Foquet, M.; Korlach, J.; Zipfel, W.; Webb. W. and Craighead, H. (2004) Focal volume confinement by submicrometer sized fluidic channels. *Anal. Chem.,* **76**, 1618-1626.

[9] Földes-Papp, Z.; Liao, S.-C. J.; Terpetschnig, E.; Kinjo, M.; Tamura, M.; Kostner, G.; Pilger, E.; Egerer, R.; Wutzler, P.; Baumann, G. and Barbieri, B. (2009) In: *Imaging and neurohistology: basic techniques,* (Doucette, R. and Walz, W. Eds., Confocal microscopy, (Ch. 13) Humana Press, Totowa, NJ, USA.

[10] Rigler, R. and Mets, Ü. (1992) Diffusion of single molecules through a Gaussian laser beam. SPIE*, Laser Spectros. Biomol.,* **1921**, 239.

[11] Földes-Papp, Z. (2005) How the molecule number is correctly quantified in two-color fluorescence cross-correlation spectroscopy: correction for cross-talk and quenching in experiments. *Curr. Pharm. Biotechnol.,* **6** (6), 437-444.

[12] Földes-Papp, Z. (2007) Fluorescence fluctuation spectroscopic approaches to the study of a single molecule diffusing in solution and a live cell without systemic drift or convection: a theoretical study. *Curr. Pharm. Biotechnol*., **8**, 261-273.

[13] Földes-Papp, Z. (2007) 'True' single-molecule molecule observations by fluorescence correlation spectroscopy and two-color fluorescence cross-correlation spectroscopy. *Exp. Mol. Pathol*., **82**, 147-155.

[14] Földes-Papp, Z. (2006) What it means to measure a single molecule in a solution by fluorescence fluctuation spectroscopy. *Exp. Mol. Pathol*., **80**, 209-218.

[15] Földes-Papp, Z.; Baumann, G.; Kinjo, M. and Tamura, M. (2005) In: *Single-phase single-molecule fluorescence correlation spectroscopy (SPSM-FCS).* (Fuchs, J. and Podda, M. Eds.), Encyclopedia of medical genomics & proteomics. Marcel Dekker, New York.

[16] Fries, J. R.; Brand, L.; Eggeling, C.; Köllner, M. and Seidel, C. A.M. (1998) Quantitative identification of different single molecules by selective time-resolved confocal fluorescence spectroscopy. *J. Phys. Chem. A*, **102**, 6601-6613.

[17] Chen, Y.; Müller, J. D.; So, P. T. C. and Gratton, E. (1999) The photon counting histogram in fluorescence fluctuation spectroscopy. *Biophys. J*., **77**, 553-567.

[18] Kask, P.; Palo, K.; Ullmann, D. and Gall, K. (1999) Fluorescence-intensity distribution analysis and its application in biomolecular detection technology. *Proc. Natl. Acad. Sci. USA*, **96**, 13756-13761.

[19] Ricka, J. and Binkert, T. (1989) Direct measurement of a distinct correlation function by fluorescence cross correlation. *Phys. Rev. A,* **39***,* 2646-2652.

[20] Schwille, P.; Meyer-Almes, F.-J. and Rigler, R. (1997) Dual-color fluorescence cross-correlation spectroscopy for multicomponent diffusional analysis in solution. *Biophys. J.*, **72**, 1878-1886.

[21] Rigler, R.; Földes-Papp, Z.; Meyer-Almes, F-J.; Sammet, C.; Völcker, M. and Schnetz, A. (1998) Fluorescence cross-correlation: a new concept for polymerase chain reaction. *J. Biotechnol.,* **63**, 97-109.

[22] Kask, P.; Palo, K.; Fay, N.; Brand, L.; Mets, Ü.; Ullmann, D.; Jungmann, J.; Pschorr, J.; Gall, K. (2000) Two-dimensional fluorescence intensity distribution analysis: *theory and applications. Biophys. J.,* **78**, 1703-1713.

[23] Chen, Y.; Tekmen, M.; Hillesheim, L.; Skinner, J.; Wu, B. and Müller, J. D. (2005) Dual-color photon-counting histogram. *Biophys. J*., **88**, 2177-2192.

[24] Eggeling, C.; Widengren, J.; Rigler, R. and Seidel, C.A.M. (1998) Photobleaching of fluorescent dyes under conditions used for single-molecule detection: Evidence of two-step photolysis. *Anal. Chem*., **70**, 2651-2659.

[25] Blom, H.; Kastrup, L. and Eggeling, C. (2006) Fluorescence fluctuation spectroscopy in reduced detection volumes. *Curr. Pharm. Biotechnol*., **7**, 51-66.

[26] Shera, E. B.; Seitzinger, N. K.; Davis. L. M.; Keller, R. A. and Soper, S. A. (1990) Detection of single fluorescent molecules. *Chem. Phys. Lett.,* **174**, 553-557.

[27] Soper, S. A.; Davis, L. M. and Shera, E. B. (1992) Detection and identification of single molecules in solution. *J. Opt. Soc. Am. B,* **9**, 1761-1769.

[28] Nyquist, R.A.; Kagel, R.O.; Putzig, C.L. and Leuger, M.A. (Eds.). (1997*) The Handbook of Infrared and Raman Spectra of Inorganic Compounds and Organic Salts.* Academic Press, San Diego, USA.

[29] Lamb, D.C.; Schenk, A.; Röcker, C. and Nienhaus, G.U. (2000) Determining chemical rate coefficients using time-gated fluorescence correlation spectroscopy. *J. Phys. Org. Chem*., **13,** 654-658.

[30] Lamb, D.C.; Schenk, A.; Röcker, C.; Scalfi-Happ, C. and Nienhaus, G.U. (2000) Sensitived enhancement in fluorescence correlation spectroscopy of multiple species using time-gated detection. *Biophys. J*., **79**, 1129-1138.

[31] Lamb, D.C.; Müller, B.K. and Bräuchle, C. (2005) Enhancing the sensitivity of fluorescence correlation spectroscopy by using time-correlated single photon counting. *Curr. Pharm. Biotechnol.,* **6**, 405-414.

[32] Wahl, M.; Erdmann, R.; Lauritsen, K. and Rahn, H.-J. (1998) Hardware solution for continuous time-resolved burst detection of single molecules in flow. *Proc. SPIE,* **3258**, 173-178.

[33] Enderlein, J. and Gregor, I. (2005) Using fluorescence lifetime for discriminating detector afterpulsing in fluorescence correlation spectroscopy. *Rev. Sci. Inst*., **76**, 033102.

[34] Aragon, S.R.; Pecora, R. (1976) Fluorescence correlation spectroscopy as a probe of molecular dynamics. *J. Chem. Phys*., **64** (4), 1791-1803.

[35] Thompson, N.L. (1991) Fluorescence correlation spectroscopy. In: Topics in Fluorescence Spectroscopy, vol 1. JR Lakowicz (Ed.), Plenum Press, New York, pp. 333-378.

[36] Persson, G.; Thyberg, P. and Widengreen, J. (2008) Modulated fluorescence correlation spectroscopy with complete time range information. *Biophys. J.,* **94**, 977-985.

[37] Li, X.; Hofmeister, W.; Shen, G.; Davis, L. and Daniel, C. (2007) (Fabrication and characterization of nanofluidics device using fused silica for single protein molecule detection). In: Proceedings of Materials and Processes for Medical Devices (*MPMD*)), Conference & Exposition, Sept. 23-25, USA.

Received: March 19, 2009 **Revised: April 20, 2009** **Accepted: April 20, 2009**